Multi-Stage Model Predictive Control with Enhanced Discrete-Time Models for Multilevel Inverters

Hoang Le*, Apparao Dekka*, Deepak Ronanki†, and Abdul R. Beig‡
*Department of Electrical and Computer Engineering, Lakehead University, Thunder Bay, Ontario, Canada
†Department of Engineering Design, Indian Institute of Technology Madras, Chennai, India
‡Advanced Power and Energy Systems, Electrical Engineering Department, Khalifa University, Abu Dhabi, UAE
E-mail: hoangvle@ieee.org, dapparao@ieee.org, dronanki@ieee.org, and balanthi.beig@ku.ac.ae

***Abstract*—Model accuracy, computational complexity, and weighting factor dependency are three primary challenges associated with multi-stage model predictive control (MS-MPC) of multilevel inverters (MLIs). Typically, existing MS-MPC employs the forward Euler integration method to discretize continuous-time models, due to the ease of implementation in real-time controllers. This approach faces a significant deterioration in computational accuracy as sampling period increases. To address this issue, this paper proposes a new formulation of MS-MPC for MLIs. Also, an enhanced discrete-time model of MLI by using Heun's integration method is proposed to implement the proposed MS-MPC, resulting in a more precise formulation and indirect minimization of common-mode voltage (CMV). Unlike the existing methods, the proposed method does not employ a cost function with weighting factor or offline selection of voltage vectors (VVs) to minimize the CMV. Furthermore, it does not increase computational complexity compared to the existing MS-MPCs. Simulation studies are conducted on a four-level MLI system to validate the efficacy of the proposed MS-MPC, and its performance is compared with the existing methods.**

***Index Terms*—Discretization method, mathematical models, model accuracy, multilevel inverter, model predictive control.**

I. Introduction

Model predictive control (MPC) methods have gained prominency in achieving multiple objectives of multilevel inverters (MLIs) and their applications [1], including renewable energy [2], [3], electrified transportation [4], [5], medium-voltage drives [6], high-voltage direct transmission systems [7], and so on. Typically, the control objectives of MLIs are achieved in a single-stage optimization for all possible switching states, which is commonly referred to as a finite control-set MPC (FCS-MPC) in the literature [8]. This method has shown a superior reference tracking at steady-state and fast response during transients compared to the linear control methods [9]. However, the mathematical models accuracy, computational complexity, and weighting factor selection affect the real-time implementation and performance of FCS-MPC methods for MLIs [10].

Traditionally, the three-phase modeling philosophy has been adopted in the formulation of FCS-MPC, resulting in a higher computational complexity, and it drastically increases with the number of voltage levels of MLIs [11]. To address this issue, the per-phase philosophy-based FCS-MPC formulation has been introduced for MLIs [12]. Irrespective of the formulation, the forward Euler integration method has been widely employed in the discretization of continuous-time (CT) models of MLIs, which affects the reference tracking performance at large sampling periods [13]. In [14], Heun's integration method has been proposed to formulate the discrete-time models for FCS-MPC, along with the per-phase implementation philosophy. This approach improves the harmonic performance and reduces the computational complexity. However, neither three-phase nor per-phase-based FCS-MPC methods have been able to escape the impact of weighting factor selection process [15]. To adjust the weighting factors dynamically, artificial neural network (ANN) [16] and adaptive approaches [17] have been proposed, but they further increases the real-time implementation complexity of FCS-MPC methods.

Alternatively, multi-stage model predictive control (MS-MPC) methods with an aim of computational complexity reduction and elimination of weighting factor dependency are well studied for MLIs [18], [19]. Depending on the number of control objectives, MS-MPC methods are designed with either two or three optimization stages by considering the redundancy of converter voltage vectors (VVs) and switching states [20], [21]. Typically, the exhaustive search is used to find the optimal VV and the corresponding switching state through multi-stage optimization process [22]. However, the exhaustive search becomes cumbersome with the increase in voltage levels of MLIs. In [23], [24], the VVs with the lowest common-mode voltage (CMV) are pre-selected offline and subsequently employed them in the optimization process. This process further reduces the computational complexity and eliminates the weighting factor dependency, but it affects the steady-state and transient performance due to the use of limited VVs in the optimization process [25]. On the other hand, the MS-MPC with indirect CMV minimization has been proposed for MLIs [26]. This approach is based on a per-phase philosophy, where the optimal voltage level for each phase is determined through an exhaustive search-based optimization process to fulfill the each phase' control objectives. It has shown a superior performance without compromising the

979-8-3315-1611-6/25/$31.00 ©2025 IEEE

transient response and computational complexity, but it leads to a high switching frequency operation.

To further simplify the MS-MPC methods, the predictive current models are reformulated in terms of predictive voltage models, thereby adapting the space vector philosophy to identify the suitable VVs for the optimization process [27]. In [28], the hysteresis comparator philosophy has been introduce to determine the optimal hexagon and sector, thereby identifying the nearest VVs and the corresponding switching states. In [29], the $g-h$ reference frame theory has been employed to identify the nearest VVs for optimization process. This philosophy has been further extended to incorporate the virtual VVs in the optimization process to address the capacitor voltage ripple reduction [30]. In [31], the sub-optimal VVs are identified based on the CMV variation and these resultant sub-optimal VVs are subsequently utilized in the cost function optimization to select the final optimal VV.

In [32], [33], the VVs are pre-selected based on the location of reference current tracking error rather than optimization process. Irrespective of the implementation philosophy, the existing MS-MPC methods are mainly targeted to reduce the computational complexity and eliminate the weighting factors, while fulfilling the control needs of MLIs and their applications. Moreover, these methods mainly use the forward Euler integration method-based models in their implementation, resulting in prediction inaccuracy as sampling period increases. To reduce impact of prediction error on the system performance, the multi-vector-based MS-MPC methods have been proposed for MLIs [34]–[36]. The use of more vector in each sampling time leads to higher device switching frequency compared to the single-vector approaches [37].

To improve the prediction accuracy, enhanced discrete-time (DT) models are proposed to implement the MS-MPC for MLIs in this article. The DT models are derived from CT models by using Heun's integration method. Moreover, the proposed MS-MPC is formulated with an indirect minimization of CMV objective to eliminate the weighting factor dependency, while maintaining a low computational burden. The enhanced DT models will also improve the harmonic performance and reduce the flying capacitor (FC) voltage ripple in MLIs. The efficacy of the proposed MS-MPC is evaluated through MATLAB simulations and its performance is further compared with the existing MS-MPC methods.

II. Modeling of the Proposed MS-MPC

The proposed MS-MPC is applied to a four-level MLI (4L-MLI), and its circuit configuration is shown in Fig. 1 [38]. The 4L-MLI is composed of eight switches (S_{w1}-S_{w8}) and two FCs (C_{w1}-C_{w2}) in each phase, where $w \in \{p, q, r\}$ denotes the ac output terminal. Table I shows the switching states corresponding to a 4L-MLI and their impact on FC voltages. Each FC is designed with a rated voltage of one-third of the dc-link voltage (V_{dc}) for a four-level operation of the inverter. The ac load is formed with a resistor (R) and an inductor (L) as shown in Fig. 1. In this article, the proposed MS-MPC is formulated to control the load currents and FC voltages

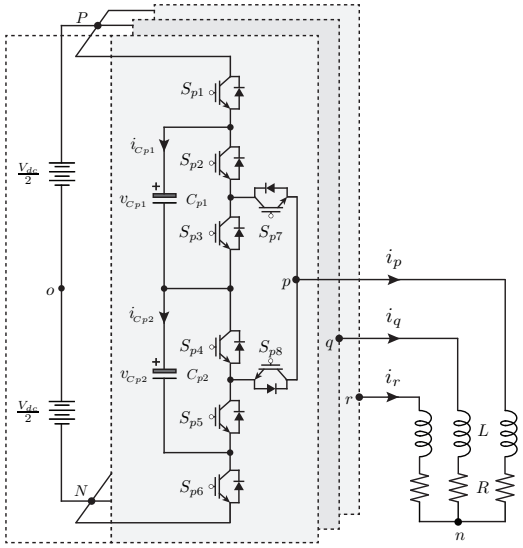

Figure 1. 4L-MLI circuit configuration [38].

of the 4L-MLI, while minimizing the CMV indirectly. The detailed formulation and mathematical models used in the implementation of the proposed MS-MPC are described as follows:

A. Formulation of Load Current Models

From Fig. 1, the CT model of the load current of phase-w can be written as [38],

$$\frac{di_w}{dt} = \frac{1}{L}\, v_{wn}(t) - \frac{R}{L}\, i_w(t) \tag{1}$$

where v_{wn} is the load voltage and i_w is the load current of phase-w.

By applying the KVL to the 4L-MLI shown in Fig. 1, the load voltage can be expressed as,

$$v_{wn}(t) = v_{wo}(t) - v_{no}(t) \tag{2}$$

where v_{wo} is the inverter voltage and v_{no} is the CMV.

To minimize the CMV indirectly in the proposed MS-MPC, the CMV objective is incorporated into load current control objective by postulating $v^*_{no}(t) = v_{no}(t) \approx 0$, leading to $v_{wo}(t) = v_{wn}(t)$ [26]. This assumption eliminates the CMV term in the load current formulation, allowing for a per-phase implementation philosophy to handle the inverter objectives.

Typically, the forward Euler method is widely used in the formulation of DT models for MS-MPC due to its simplicity and ease of implementation in real-time controllers. However, the accuracy of these models degrades as the sampling period increases and they are given as,

$$i^p_w(h+1) = \left(1 - \frac{T_s\, R}{L}\right)\, i_w(h) + \frac{T_s}{L}\, v_{wo}(h) \tag{3}$$

where T_s is the sampling period.

To enhance model accuracy, Heun's integration method is employed to discretize the CT model in (1) [13]. The resultant

Table I
SWITCHING STATES OF A FOUR-LEVEL MLI [38]

$\mathbf{S}_w$	S_{w1}	S_{w2}	S_{w3}	S_{w4}	S_{w5}	S_{w6}	S_{w7}	S_{w8}	v_{Cw1}	v_{Cw2}	v_{wN}
0	0	0	0	0	1	1	0	1	No Change	No Change	0
1	1	0	0	0	1	0	0	1	Charge ($i_w > 0$)	Charge ($i_w > 0$)	$V_{dc} - v_{Cw1} - v_{Cw2} = \frac{V_{dc}}{3}$
	0	0	0	1	0	1	0	1	No Change	Discharge ($i_w > 0$)	$v_{Cw2} = \frac{V_{dc}}{3}$
2	0	1	0	0	0	1	1	0	Discharge ($i_w > 0$)	Discharge ($i_w > 0$)	$v_{Cw1} + v_{Cw2} = \frac{2\,V_{dc}}{3}$
	1	0	1	0	0	0	1	0	Charge ($i_w > 0$)	No Change	$V_{dc} - v_{Cw1} = \frac{2\,V_{dc}}{3}$
3	1	1	0	0	0	0	1	0	No Change	No Change	V_{dc}

DT model of the load current is given as,

$$i_w^p(h+1) = \left(\frac{1}{2}\left(\frac{T_s\,R}{L}\right)^2 - \frac{T_s\,R}{L} + 1\right) i_w(h) + \left(\frac{T_s}{L} - \frac{R}{2}\left(\frac{T_s}{L}\right)^2\right) v_{wo}(h) \tag{4}$$

Considering the switching states given in Table I, the 4L-MLI output voltage with respect to the dc-link mid-point (o) can be written as,

$$\begin{aligned} v_{wo}(h) &= \mathbf{S}_w\,(\mathbf{S}_w - 1)\,(3 - \mathbf{S}_w)\frac{v_{Cw1}(h)}{2} \\ &+ \mathbf{S}_w\,(3 - \mathbf{S}_w)\frac{v_{Cw2}(h)}{2} \\ &+ \mathbf{S}_w\,(\mathbf{S}_w - 1)\,(\mathbf{S}_w - 2)\frac{V_{dc}}{6} - \frac{V_{dc}}{2} \end{aligned} \tag{5}$$

where $\mathbf{S}_w$ is 4L-MLI phase voltage level.

The cost function for the load current optimization process is formulated as,

$$J_{w1} = \left(\widehat{i}_w^*(h+1) - i_w^p(h+1)\right)^2 \tag{6}$$

B. Formulation of FC Voltage and Current Models

According to circuit configuration in Fig. 1, the 4L-MLI is composed of 2 FCs in each phase. The CT model of the kth FC voltage in phase-w is given as,

$$\frac{d\,v_{Cwk}}{dt} = \frac{i_{Cwk}(t)}{C_{wk}} \tag{7}$$

where v_{Cwk} is the FC voltage, i_{Cwk} is the FC current, C_{wk} is the capacitance of FCs, and $k \in \{1, 2\}$ is the FC index number.

The DT model of predictive FC voltage based on the forward Euler integration method is given as [26],

$$v_{Cwk}^p(h+1) = v_{Cwk}(h) + T_s\,\frac{i_{Cwk}(h)}{C_{wk}} \tag{8}$$

To obtain a more precise model, Heun's integration method is applied to the CT model in (7) [13], and resultant model is given as,

$$v_{Cwk}^p(h+1) = v_{Cwk}(h) + T_s\left(\frac{i_{Cwk}(h)}{2\,C_{wk}} + \frac{i_{Cwk}(h+1)}{2\,C_{wk}}\right) \tag{9}$$

The predictive FC currents at the (h)th sampling instant are given according to Table I as,

$$\begin{aligned} i_{Cw1}(h) &= (S_{w1} - S_{w2})\,i_w(h) \\ i_{Cw2}(h) &= (S_{w5} - S_{w6})\,i_w(h) \end{aligned} \tag{10}$$

Similarly, the FC currents at the $(h+1)$th sampling instant can be written as,

$$\begin{aligned} i_{Cw1}(h+1) &= (S_{w1} - S_{w2})\,i_w^{op}(h+1) \\ i_{Cw2}(h+1) &= (S_{w5} - S_{w6})\,i_w^{op}(h+1) \end{aligned} \tag{11}$$

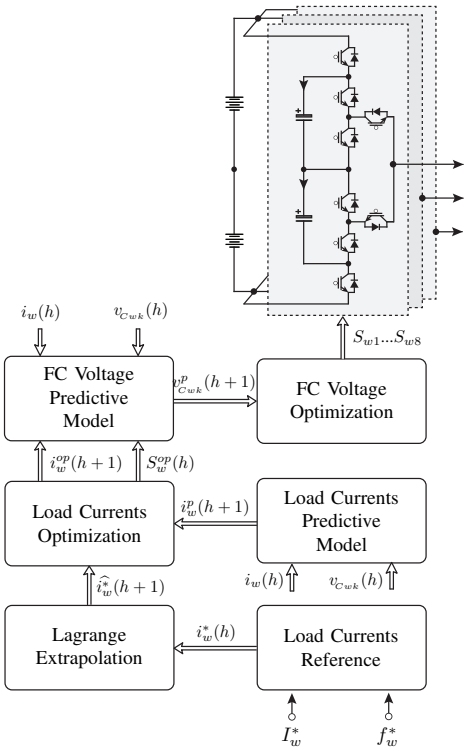

Figure 2. Block diagram of the proposed MS-MPC.

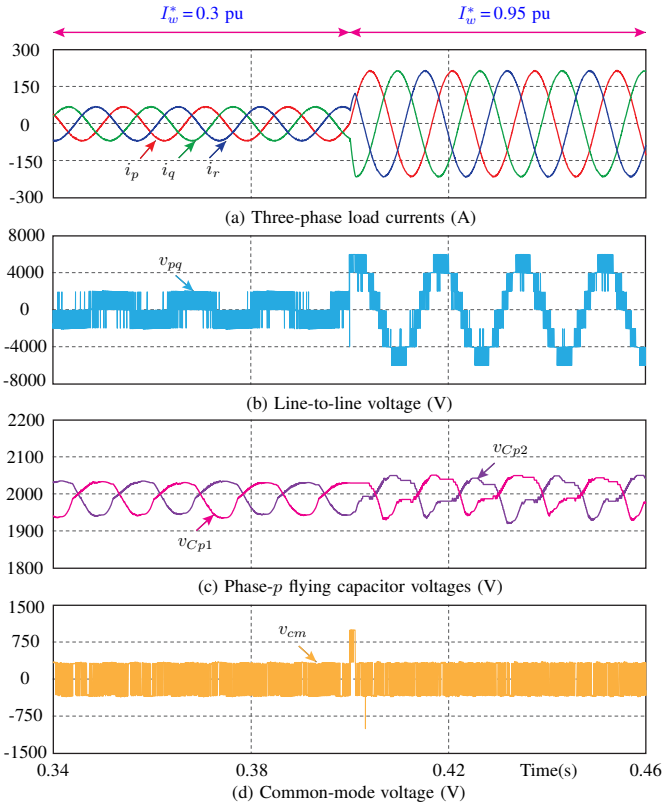

Figure 3. Proposed MS-MPC performance with current magnitude step-change at $f_w^* = 60$ Hz.

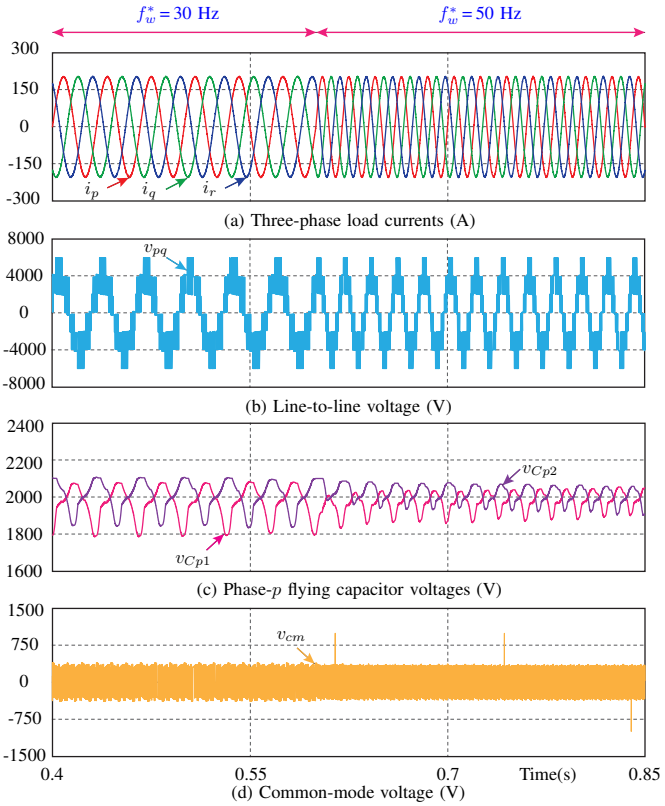

Figure 4. Proposed MS-MPC performance with frequency step-change at $I_w^* = 0.9$ pu.

Table II
ANALYSIS WITH I_w^* VARIATION AT $f_w^* = 60$ HZ

Performance index	$I_w^* = 0.3$ pu	$I_w^* = 0.95$ pu
%THD$_i$	2.41	0.79
%THD$_v$	101.88	31.06
Δv_C (V)	97	132

Table III
ANALYSIS WITH f_w^* VARIATION AT $I_w^* = 0.9$ PU

Performance index	$f_w^* = 30$ Hz	$f_w^* = 50$ Hz
%THD$_i$	0.87	0.86
%THD$_v$	38.30	34
Δv_C (V)	280	150

where $i_w^{op}(h+1)$ is the optimal value of phase-w current corresponding to the optimal voltage level of S_w^{op}.

The cost function (J_{w2}) is formulated with the predictive and reference FC voltages and it is given as

$$J_{w2} = \left(v_{Cwk}^*(h+1) - v_{Cwk}^p(h+1)\right)^2 \tag{12}$$

where v_{Cwk}^* represents reference FC voltage, which is set to $V_{dc}/3$ in a 4L-MLI.

III. IMPLEMENTATION OF THE PROPOSED MS-MPC

The proposed MS-MPC method for a 4L-MLI is implemented in two stages and their design steps are depicted in Fig. 2. In this method, the load current references (i_w^*) at the hth sampling instant are generated with a specified magnitude of I_w^* and a frequency of f_w^*, and they are given as,

$$i_w^*(h) = I_w^* \times sin(2\pi f_w^* + \theta_w) \tag{13}$$

where $\theta_w \in \left\{0, \frac{2\pi}{3}, \frac{4\pi}{3}\right\}$ denotes phase angles.

Through Lagrange extrapolation, the load current references are extrapolated to the $(h+1)$th sampling instant from (h)th sampling instant, and they are given as,

$$\begin{aligned}\widehat{i_w^*}(h+1) = {} & 4\,i_w^*(h) - 6\,i_w^*(h-1) \\ & + 4\,i_w^*(h-2) - i_w^*(h-3)\end{aligned} \tag{14}$$

The load currents are predicted at the $(h+1)$th sampling instant by using (4). These currents are used in the cost function (6), together with the reference load currents. Each phase cost function is evaluated for a total of 4 voltage levels to determine the optimal voltage level (S_w^{op}) and the corresponding optimal load current value (i_w^{op}). These values together with the measured FC voltages are used in the prediction process of FC voltages given in (9)–(11). The predicted and reference FC voltages are used to form a cost function J_{w2} in (12). This cost function is evaluated for switching states corresponding to

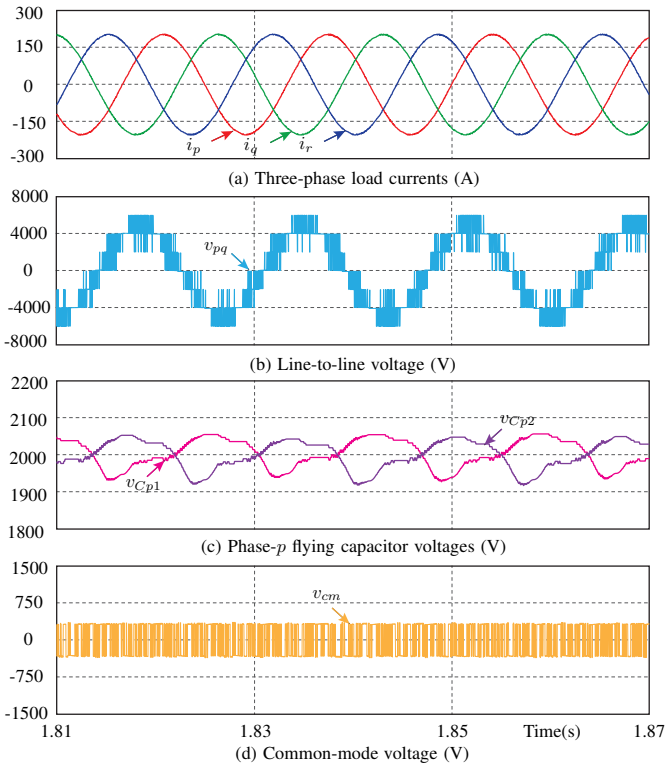

Figure 5. Existing MS-MPC performance at $I_w^* = 0.9$ pu and $f_w^* = 60$ Hz.

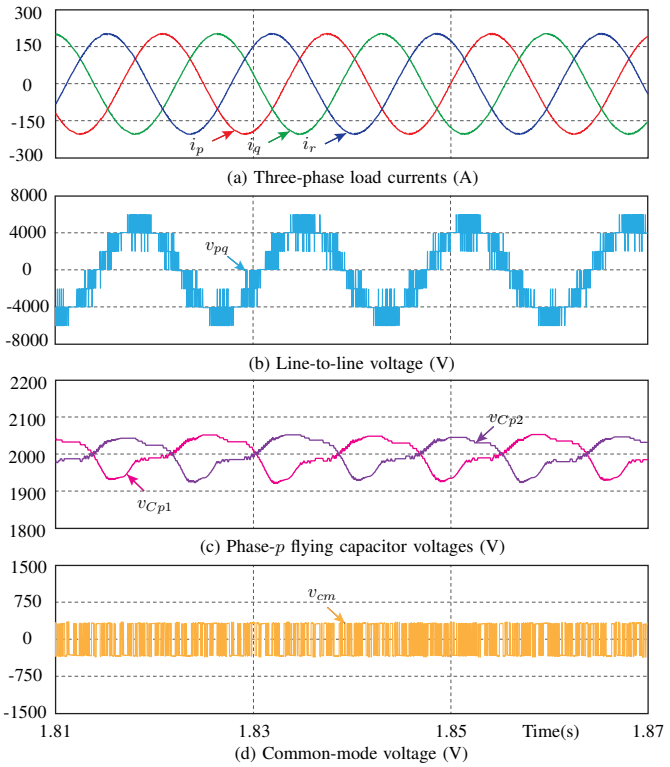

Figure 6. Proposed MS-MPC performance at $I_w^* = 0.9$ pu and $f_w^* = 60$ Hz.

the optimal voltage level only. Finally, the optimum switching state corresponding to the smallest cost value is then selected and applied to the 4L-MLI.

IV. Simulation Results and Analysis

The performance of the proposed MS-MPC under various working scenarios are validated on MATLAB simulation environment. The 4L-MLI is designed with the following specifications: rated power $(S_o) = 1.1$ MVA, rated voltage (line-to-line, rms) $(v_o) = 4000$ V, dc-link voltage $(V_{dc}) = 6000$ V, FC capacitance $(C_{wk}), = 1100\,\mu$F, rated FC voltage $(v_{Cwk}^*) = 2000$ V, load resistance $(R) = 13\,\Omega$, load inductance $(L) = 13$ mH, and sampling period $(T_s) = 40\,\mu$s. Performance metrics used to evaluate the system performance include current harmonic distortion (%THD$_i$), voltage harmonic distortion (%THD$_v$), and FC voltage ripple (ΔV_c).

Fig. 3 shows the performance of the proposed MS-MPC during a step change in current magnitude from $I_w^* = 0.3$ pu to 0.95 pu, with an operating frequency (f_w^*) of 60 Hz. The results show that, regardless of working conditions, the three-phase load currents are perfectly sinusoidal with a %THD$_i$ of 2.41 and 0.79 at $I_w^* = 0.3$ pu and 0.95 pu, respectively, as shown in Fig. 3(a) and summarized in Table II. With increasing current magnitude, the line voltage rises from 3 steps to 7 steps (see Fig. 3(b)), resulting in a decrease in the %THD$_v$ from 101.88 to 31.06, as shown in Table II. Throughout the process, FC voltages are perfectly regulated at their rated values of 2000 V each as shown in Fig. 3(c). They have a ΔV_c of 97 V at $I_w^* = 0.3$ pu and 132 V at $I_w^* = 0.95$ pu. The results indicate that the higher current magnitude leads to a greater FC voltages ripple. Regardless of operating conditions, the 4L-MLI produces the least CMV at 358 V (peak) as shown in Fig. 3(d), and there is a spike in voltage at the moment of transient (at $t = 0.4$ s).

Table IV
Comparison Analysis of Existing and Proposed MS-MPC at $I_w^* = 0.9$ pu and $f_w^* = 60$ Hz

Performance index	Existing MS-MPC	Proposed MS-MPC
%THD$_i$	0.87	0.81
%THD$_v$	34.86	33.82
Δv_C (V)	138	129

The performance of the proposed MS-MPC under the step change in frequency is shown in Fig. 4. In this study, the reference frequency (f_w^*) changes from 30 Hz to 50 Hz at $t = 0.6$ s while maintaining I_w^* at 0.9 pu. The results show that, regardless of operating conditions, the three-phase load currents have a %THD$_i$ of 0.87 at 30 Hz and 0.86 at 50 Hz, as shown in Fig. 4(a), and the same details are given in Table III. It is also observed that the change in frequency has no impact on the %THD$_i$ performance of the proposed MS-MPC. The line voltage remains 7 steps throughout the operation, and it has a %THD$_v$ of 38.30 and 34 at 30 Hz and 50 Hz, respectively, as shown in Fig. 4(b). Throughout the operation, each FC voltage is regulated at 2000 V as shown in

Fig. 4(c). These FCs have a ΔV_c of 280 V and 150 V at 30 Hz and 50 Hz, respectively. During the process, the proposed MS-MPC maintains the minimal CMV at 358 V (peak), as shown in Fig. 4(d).

To evaluate the effectiveness of the proposed MS-MPC, its performance is compared with the existing MS-MPC (forward Euler-based) [26], and the results are shown in Figs. 5 and 6. Irrespective of control methods, the three-phase load currents are perfectly sinusoidal as shown in Figs. 5(a) and 6(a). However, while the existing MS-MPC has a $\%\text{THD}_i$ of 0.87, the proposed MS-MPC produces a lower $\%\text{THD}_i$ of 0.81, as shown in Table IV. The line voltage has 7 steps with a $\%\text{THD}_v$ of 34.61 and 33.82 for existing MS-MPC and proposed MS-MPC, respectively, as shown in Figs. 5(b) and 6(b). Regardless of control techniques, FC voltages are consistently maintained at their reference values with a ΔV_c of 138 V for the existing method (see Fig. 5(c)) and a reduced ΔV_c of 129 V for the proposed MS-MPC (see Fig. 6(c)). During the process, both methods produce the same CMV with 358 V (peak), as shown in Figs. 5(d) and 6(d). It is interesting to note that both methods require the same execution time.

V. Conclusions

In this paper, an enhanced DT models using Heun's integration method for MS-MPC is proposed and applied to a 4L-MLI. The detailed formulation of DT models of the 4L-MLI with Heun's method and implementation steps of the proposed MS-MPC are also presented. The proposed MS-MPC is also studied on a 4L-MLI through MATLAB simulations under various operating conditions. The results show that the proposed method effectively reduces the current and voltage harmonic distortions and FC voltage ripples, while producing the lowest CMV. Furthermore, this approach does not increase computational complexity compared to existing MS-MPC. Overall, the proposed MS-MPC shows a superior performance with the enhanced DT models over the forward Euler method-based models, and it is highly suitable for MLI-fed electric motor drive applications.

References

[1] P. Karamanakos, E. Liegmann, T. Geyer, and R. Kennel, "Model predictive control of power electronic systems: Methods, results, and challenges," *IEEE Open J. Ind. Appl.*, vol. 1, pp. 95–114, 2020.

[2] Y. Arias-Esquivel, R. Cárdenas, M. Diaz, and L. Tarisciotti, "Continuous control set model predictive control of a hybrid modular multilevel converter for wind energy applications," *IEEE Trans. Ind. Electron.*, vol. 71, no. 11, pp. 14 287–14 297, Nov 2024.

[3] T. Jin, X. Shen, T. Su, and R. C. C. Flesch, "Model predictive voltage control based on finite control set with computation time delay compensation for pv systems," *IEEE Trans. Energy Convers.*, vol. 34, no. 1, pp. 330–338, Mar 2019.

[4] D. Ronanki and H. Karneddi, "Electric vehicle charging infrastructure: Review, cyber security considerations, potential impacts, countermeasures, and future trends," *IEEE J. Emerg. Sel. Topics Power Electron.*, vol. 12, no. 1, pp. 242–256, Feb 2024.

[5] A. Andersson and T. Thiringer, "Assessment of an improved finite control set model predictive current controller for automotive propulsion applications," *IEEE Trans. Ind. Electron.*, vol. 67, no. 1, pp. 91–100, Jan 2020.

[6] H. Le, A. Dekka, and D. Ronanki, "Modeling and control of a new five-level converter for medium-voltage drive systems," *IEEE Trans. Transport. Electrific.*, vol. 10, no. 2, pp. 3782–3791, Jun 2024.

[7] J. Carmona Sánchez, O. Marjanovic, M. Barnes, and P. R. Green, "Secondary model predictive control architecture for vsc-hvdc networks interfacing wind power," *IEEE Trans. Power Del.*, vol. 35, no. 5, pp. 2329–2341, Oct 2020.

[8] P. Karamanakos, T. Geyer, and R. Kennel, "On the choice of norm in finite control set model predictive control," *IEEE Trans. Power Electron.*, vol. 33, no. 8, pp. 7105–7117, 2018.

[9] J. Rodriguez, C. Garcia, A. Mora, S. A. Davari, J. Rodas, D. F. Valencia, M. Elmorshedy, F. Wang, K. Zuo, L. Tarisciotti, F. Flores-Bahamonde, W. Xu, Z. Zhang, Y. Zhang, M. Norambuena, A. Emadi, T. Geyer, R. Kennel, T. Dragicevic, D. A. Khaburi, Z. Zhang, M. Abdelrahem, and N. Mijatovic, "Latest advances of model predictive control in electrical drives–part ii: Applications and benchmarking with classical control methods," *IEEE Trans. Power Electron.*, vol. 37, no. 5, pp. 5047–5061, May 2022.

[10] I. Harbi, J. Rodriguez, E. Liegmann, H. Makhamreh, M. L. Heldwein, M. Novak, M. Rossi, M. Abdelrahem, M. Trabelsi, M. Ahmed, P. Karamanakos, S. Xu, T. Dragičević, and R. Kennel, "Model-predictive control of multilevel inverters: Challenges, recent advances, and trends," *IEEE Trans. Power Electron.*, vol. 38, no. 9, pp. 10 845–10 868, Sept 2023.

[11] N. Chai, W. Tian, X. Gao, J. Rodriguez, M. L. Heldwein, and R. Kennel, "Three-phase model-based predictive control methods with reduced calculation burden for modular multilevel converters," *IEEE J. Emerg. Sel. Topics Power Electron.*, vol. 10, no. 6, pp. 7037–7048, Dec 2022.

[12] A. Bahrami, M. Norambuena, M. Narimani, and J. Rodriguez, "Model predictive current control of a seven-level inverter with reduced computational burden," *IEEE Trans. Power Electron.*, vol. 35, no. 6, pp. 5729–5740, Jun 2020.

[13] H. Le, A. Dekka, D. Ronanki, and J. Rodriguez, "A new predictive current control with reduced current tracking error and switching frequency for multilevel inverters," *IEEE Trans. Power Electron.*, vol. 38, no. 9, pp. 10 798–10 809, Sept 2023.

[14] D. Prajapati, A. Dekka, D. Ronanki, and J. Rodriguez, "Low-complexity heun's method-based fcs-mpc with reduced common-mode voltage for a five-level inverter," *IEEE Trans. Power Electron.*, vol. 39, no. 3, pp. 3329–3338, 2024.

[15] E. Zerdali, M. Rivera, and P. Wheeler, "A review on weighting factor design of finite control set model predictive control strategies for ac electric drives," *IEEE Trans. Power Electron.*, vol. 39, no. 8, pp. 9967–9981, Aug 2024.

[16] T. Dragičević and M. Novak, "Weighting factor design in model predictive control of power electronic converters: An artificial neural network approach," *IEEE Trans. Ind. Electron.*, vol. 66, no. 11, pp. 8870–8880, Nov 2019.

[17] C. Tang and T. Thiringer, "A model predictive control method with adaptive weighting factors for enhancing performance of modular multilevel converters," *IEEE J. Emerg. Sel. Topics Power Electron.*, vol. 12, no. 4, pp. 3887–3899, Aug 2024.

[18] Y. Yang, H. Wen, M. Fan, M. Xie, S. Peng, M. Norambuena, and J. Rodriguez, "Computation-efficient model predictive control with common-mode voltage elimination for five-level anpc converters," *IEEE Trans. Transport. Electrific.*, vol. 6, no. 3, pp. 970–984, Sept 2020.

[19] W. Wu, D. Wang, and L. Liu, "A multi-layer sequential model predictive control of three-phase two-leg seven-level t-type nested neutral point clamped converter without weighting factors," *IEEE Access*, vol. 7, pp. 162 735–162 746, 2019.

[20] Y. Yang, R. Chen, M. Fan, Y. Xiao, X. Zhang, M. Norambuena, and J. Rodriguez, "Improved model predictive current control for three-phase three-level converters with neutral-point voltage ripple and common mode voltage reduction," *IEEE Trans. Energy Convers.*, vol. 36, no. 4, pp. 3053–3062, Dec 2021.

[21] H. Lin, S. Niu, Y. Chen, W. Wang, X. Tang, P. Zhang, and Z. Yuan, "Three-stage duty cycle-based deadbeat predictive torque control for three-phase spmsms with cmv reduction," *IEEE Trans. Power Electron.*, vol. 38, no. 9, pp. 11 385–11 398, Sept 2023.

[22] Y. Zhang and W. Xie, "Low complexity model predictive control-single vector-based approach," *IEEE Trans. Power Electron.*, vol. 29, no. 10, pp. 5532–5541, Oct 2014.

[23] N. S. P. Musunuru and S. Srirama, "Cascaded predictive control of a single power supply-driven four-level open-end winding induction motor drive without weighting factors," *IEEE J. Emerg. Sel. Topics Power Electron.*, vol. 9, no. 3, pp. 2858–2867, Jun 2021.

[24] U. R. Muduli, A. R. Beig, R. K. Behera, K. A. Jaafari, and J. Y. Alsawalhi, "Predictive control with battery power sharing scheme for

dual open-end-winding induction motor based four-wheel drive electric vehicle," *IEEE Trans. Ind. Electron.*, vol. 69, no. 6, pp. 5557–5568, Jun 2022.

[25] D. Prajapati, A. Dekka, D. Ronanki, and J. Rodriguez, "High-performance sequential model predictive control of a four-level inverter for electric transportation applications," *IEEE J. Emerg. Sel. Topics Ind. Electron.*, vol. 5, no. 1, pp. 253–262, Jan 2024.

[26] H. Le, A. Dekka, and D. Ronanki, "Model predictive control with inherent cmv reduction capability for multilevel inverters," *IEEE Trans. Ind. Electron.*, vol. 71, no. 7, pp. 6730–6737, 2024.

[27] Y. Wang, Y. Yang, S. Chen, R. Chen, J. Hu, W. Wu, Y. Wang, H. Yang, L. Zhou, and J. Rodriguez, "An improved model predictive voltage control with reduced computational burden for t-type three-phase three-level inverters," *IEEE Trans. Power Electron.*, vol. 39, no. 2, pp. 2115–2127, Feb 2024.

[28] D. Zhou, L. Ding, and Y. Li, "Two-stage optimization-based model predictive control of 5l-anpc converter-fed pmsm drives," *IEEE Trans. Ind. Electron.*, vol. 68, no. 5, pp. 3739–3749, 2021.

[29] Y. Li, F. Diao, and Y. Zhao, "A generic two-vector model predictive control for hybrid multilevel converters," *IEEE J. Emerg. Sel. Topics Power Electron.*, vol. 9, no. 5, pp. 6008–6018, Oct 2021.

[30] Y. Li and Y. Zhao, "A virtual space vector model predictive control for a seven-level hybrid multilevel converter," *IEEE Trans. Power Electron.*, vol. 36, no. 3, pp. 3396–3407, March 2021.

[31] Z. Ni, A. H. Abuelnaga, Y. Pan, A. Elezab, O. Zayed, M. Narimani, and J. Rodriguez, "A new mpc formulation based on suboptimal voltage vectors for multilevel inverters," *IEEE J. Emerg. Sel. Topics Power Electron.*, vol. 10, no. 6, pp. 7261–7270, Dec 2022.

[32] M. S. R. Saeed, W. Song, B. Yu, A.-R. Youssef, E. E. M. Mohamed, and A. I. M. Ali, "Computationally efficient pre-selection-based model predictive control for five-phase three-level drives," *IEEE Trans. Transport. Electrific.*, pp. 1–1, 2024.

[33] M. L. Parvathy and V. K. Thippiripati, "A simplified voltage vector preselection-based multivector predictive current control for improved torque performance of pmsm drive," *IEEE Trans. Power Electron.*, vol. 38, no. 7, pp. 8775–8785, Jul 2023.

[34] Y. Yang, J. Pan, H. Wen, Z. Zhang, Z. Ke, and L. Xu, "Double-vector model predictive control for single-phase five-level actively clamped converters," *IEEE Trans. Transport. Electrific.*, vol. 5, no. 4, pp. 1202–1213, Dec 2019.

[35] X. Li, Z. Xue, L. Zhang, and W. Hua, "A low-complexity three-vector-based model predictive torque control for spmsm," *IEEE Trans. Power Electron.*, vol. 36, no. 11, pp. 13 002–13 012, Nov 2021.

[36] I. Harbi, M. Ahmed, C. M. Hackl, J. Rodriguez, R. Kennel, and M. Abdelrahem, "Low-complexity dual-vector model predictive control for single-phase nine-level anpc-based converter," *IEEE Trans. Power Electron.*, vol. 38, no. 3, pp. 2956–2971, Mar 2023.

[37] W. Hua, F. Chen, W. Huang, G. Zhang, W. Wang, and W. Xia, "Multivector-based model predictive control with geometric solution of a five-phase flux-switching permanent magnet motor," *IEEE Trans. Ind. Electron.*, vol. 67, no. 12, pp. 10 035–10 045, Dec 2020.

[38] H. Le, A. Dekka, D. Ronanki, and J. Rodriguez, "Predictive current control of a new four-level voltage source inverter," in *2022 IEEE International Conference on Power Electronics, Drives and Energy Systems (PEDES)*, 2022, pp. 1–5.